

1 **Reaction Rebalancing: A Novel**
2 **Approach to Curating Reaction**
3 **Databases**

4 Tieu-Long Phan^{1,2*†}, Klaus Weinbauer^{1,3†}, Thomas Gärtner³,
5 Daniel Merkle^{4,2}, Jakob L. Andersen², Rolf Fagerberg²,
6 Peter F. Stadler^{1,5,6,7,8,9}

7 ¹Bioinformatics Group, Department of Computer Science &
8 Interdisciplinary Center for Bioinformatics & School for Embedded and
9 Composite Artificial Intelligence (SECAI), Leipzig University,
10 Härtelstraße 16–18, D-04107 Leipzig, Germany.

11 ²Department of Mathematics and Computer Science, University of
12 Southern Denmark, DK-5230 Odense M, Denmark .

13 ³Machine Learning Research Unit, TU Wien Informatics,
14 Erzherzog-Johann-Platz 1 (FB02), A-1040 Wien, Austria.

15 ⁴Faculty of Technology, Bielefeld University, Postfach 10 01 31, D-33501
16 Bielefeld, Germany.

17 ⁵Max Planck Institute for Mathematics in the Sciences, Inselstraße 22,
18 D-04103 Leipzig, Germany.

19 ⁶Department of Theoretical Chemistry, University of Vienna,
20 Währingerstraße 17, A-1090 Wien, Austria.

21 ⁷Facultad de Ciencias, Universidad Nacional de Colombia, Bogotá,
22 Colombia.

23 ⁸Center for non-coding RNA in Technology and Health, University of
24 Copenhagen, Ridebanevej 9, DK-1870 Frederiksberg, Denmark.

25 ⁹Santa Fe Institute, 1399 Hyde Park Rd., Santa Fe, NM 87501, USA.

26 ^{*}Corresponding author(s). E-mail(s): long.tieu.phan@uni-leipzig.de;

27 Contributing authors: klaus@bioinf.uni-leipzig.de;

28 thomas.gaertner@tuwien.ac.at; daniel.merkle@uni-bielefeld.de;

29 jlandersen@imada.sdu.dk; rolf@imada.sdu.dk;

30 studla@bioinf.uni-leipzig.de;

Abstract

Purpose: Reaction databases are a key resource for a wide variety of applications in computational chemistry and biochemistry, including Computer-aided Synthesis Planning (CASP) and the large-scale analysis of metabolic networks. The full potential of these resources can only be realized if datasets are accurate and complete. Missing co-reactants and co-products, i.e., unbalanced reactions, however, are the rule rather than the exception. The curation and correction of such incomplete entries is thus an urgent need.

Methods: The SynRBL framework addresses this issue with a dual-strategy: a rule-based method for non-carbon compounds, using atomic symbols and counts for prediction, alongside a Maximum Common Subgraph (MCS)-based technique for carbon compounds, aimed at aligning reactants and products to infer missing entities.

Results: The rule-based method exceeded 99% accuracy, while MCS-based accuracy varied from 81.19% to 99.33%, depending on reaction properties. Furthermore, an applicability domain and a machine learning scoring function were devised to quantify prediction confidence. The overall efficacy of this framework was delineated through its success rate and accuracy metrics, which spanned from 89.83% to 99.75% and 90.85% to 99.05%, respectively.

Conclusion: The SynRBL framework offers a novel solution for recalibrating chemical reactions, significantly enhancing reaction completeness. With rigorous validation, it achieved groundbreaking accuracy in reaction rebalancing. This sets the stage for future improvement in particular of atom-atom mapping techniques as well as of downstream tasks such as automated synthesis planning.

Keywords: reaction databases, unbalanced reactions, data curation, SynRBL, rules, maximum-common-subgraph

1 Introduction

Large-scale reaction databases such as the United States Patent and Trademark Office (USPTO) database [1] and the commercial database Reaxys [2] catalogue millions of chemical reactions and serve to enable data-driven approaches in chemistry. Reaxys, hosting over 55 million manually curated reactions, has become a cornerstone for deploying deep-learning neural networks in retrosynthesis [3, 4, 5, 6, 7], robotic chemistry [8], and the determination of optimal reaction conditions [9].

USPTO is the largest public collection of chemical reactions, comprising more than 3 million entries mined from approximately 9 million US patents covering 1976 to 2016. Its impact on cheminformatics and synthetic chemistry is significant, and as a public resource, it has particular impact in methods development. It plays a pivotal role in the advancement of reaction database analysis [10], forward [11, 12, 13] and backward [14] synthesis prediction, and yield prediction [15, 16]. The database has been instrumental

71 also in reaction classification [17, 18], atom-to-atom mapping [19, 20], and synthesis
72 rule clustering [21].

73 Despite the rapid advancements of databases, data quality remains a significant
74 issue in particular for machine learning applications in chemistry [22]. A particularly
75 serious problem is that omission of co-reactants or co-products. For example, less than
76 12% of the single step reactions in Reaxys analyzed to study the exploration history
77 of chemical space [23] were balanced. This problem has multiple roots, including his-
78 torical and procedural practices. These deficiencies are attributed to the limitations
79 of text mining, which struggles with the variability of publication formats [24], and to
80 errors introduced during manual data curation [25].

81 Many data-driven applications therefore attempt to ignore the fact that many or
82 most reactions are unbalanced and operate directly on such imperfect reaction data.
83 This is in particular the case of atom-atom mapping methods. RXNMapper [20] and
84 GraphormerMapper [26] apply machine learning for reaction mapping and atom embed-
85 ding improvements, respectively, without directly addressing reaction imbalances.
86 Jaworski’s rule-based atom-atom-mapper [19], on the other hand, uses graph-theoretic
87 considerations that introduce small molecules to achieve stoichiometric balance before
88 atom correspondences are inferred. GraphormerMapper was reported to show enhanced
89 performance on the Golden dataset of manually mapped and curated reactions [27].
90 Its efficacy on unbalanced reactions remains undocumented.

91 Several tools dedicated to balancing reactions have become available. CGRTools
92 offers a rule-based method for rebalancing reactions by adding small molecules, which
93 however has limited success in achieving perfect balance [28]. A hybrid workflow
94 [29] combines ChemBalancer’s heuristic methods and ChemMLM’s machine learning to
95 enhance molecule prediction. While ChemBalancer focuses on reaction completion,
96 lacking precise accuracy metrics, ChemMLM shows promise with small molecules but
97 struggles with complex structures [29].

98 The SynRBL framework for rebalancing reactions, which we introduce here, com-
99 bines two methods: a rule-based approach for missing non-carbon compounds, i.e.
100 compounds without carbon atoms like H₂O or HCl, and a graph-theoretic approach
101 for missing carbon structures. The rule-based method uses atomic symbols and counts
102 to determine if reactions are balanced, decomposing molecules into ions to minimize
103 redundancy and employing a search strategy that leverages a rule library to identify
104 missing molecules.

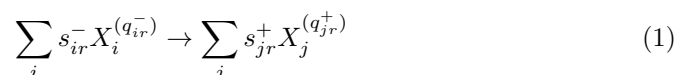
105 For carbon compounds, we consider a maximum common subgraph (MCS) prob-
106 lem. This family of combinatorial optimization problems plays an important role in
107 structural comparisons in chemistry and biology [30]. It underlies similarity searches
108 vital to the preliminary phases of drug discovery, offering metrics for molecular struc-
109 ture similarity based on MCS dimensions, in alignment with the principle of similar
110 properties [31, 32]. Beyond similarity assessment, MCS analysis is integral to cluster-
111 ing processes [33, 34, 35], the identification of matched molecular pairs [36], reaction
112 mapping [37, 38], and the alignment of molecules [39]. MCS problems come in two
113 flavors, both of which are NP-hard [40]. These two flavors are the maximum common
114 induced subgraph (MCIS), which focuses on atom count, and the maximum common
115 edge subgraph (MCES), which focuses on edge count. They give notable differences

116 in the analyses of dissimilar molecules [41]. Our MCS-based approach targets carbon
117 compound gaps and reactions beyond the rule-based method’s scope by aligning reac-
118 tants and products to pinpoint and merge non-aligned segments, generating missing
119 compounds. An iterative technique proceeding by overlapping molecules one at a time
120 and isolating non-overlapping regions for efficient alignment in subsequent rounds is
121 introduced to reduce computational costs.

122 2 Method

123 2.1 Notation and Preliminaries

124 Every chemical reaction r can be written in the form



125 where $s_{ir}^- \geq 0$ and $s_{jr}^+ \geq 0$ are the stoichiometric coefficients of compounds X_i and X_j
126 appearing as a reactant and as product, respectively. The superscripts (q_{ir}^-) and (q_{jr}^+)
127 indicate the charge of the compounds X_i and X_j among the reactants and products,
128 respectively. A molecule does not appear as a reactant or product if its stoichiometric
129 coefficient vanishes, i.e., if $s_{ir}^- = 0$ and $s_{jr}^+ = 0$, respectively. Since we consider only a
130 single fixed reaction in the following, we drop the index r from here on.

131 Every compound X_i has a well-defined composition expressed by its sum formula.
132 We write n_{ai} for the number of atoms of type a in compound i . The equilibrium of
133 chemical reactions, grounded in the Law of Conservation of Mass by Antoine Lavoisier
134 [42], stipulates that all reactions r are *balanced* in the sense that the total number n_{ar}^-
135 of atoms of type a in the reactants equals the total number n_{ar}^+ of atoms of type a in
136 the products, i.e.,

$$n_a^- := \sum_i n_{ai} s_i^- = \sum_i n_{ai} s_i^+ =: n_a^+ \quad (2)$$

137 Similarly, the Law of Conservation of Charge ensures the constancy of total charge,
138 crucial in redox and ionic reactions, i.e., it ensures that for every reaction

$$q^- := \sum_i s_i^- q_i^- = \sum_i s_i^+ q_i^+ =: q^+ \quad (3)$$

139 In organic chemistry, carbon balancing (expressed as $n_C^- = n_C^+$), is essential for tracking
140 carbon atoms in bond formations or cleavages, highlighting the significance of carbon
141 atom accounting [43]. Balancing carbons is in practice more challenging because the
142 imbalance is usually much larger compared to the atoms found in functional groups
143 because larger organic molecules are not represented in the reaction data.

144 The task of reaction balancing can be expressed as follows. If a reaction is *unbal-*
145 *anced*, i.e., if $n_a^- \neq n_a^+$ for one or more atom types a , find a set of reactants $\{X_k^{(q_k^-)}\}$
146 and a set of products $\{X_l^{(q_l^+)}\}$ with non-zero stoichiometric coefficients t_k^- and t_l^+ such

147 that

$$n_a^- + \sum_k n_{ak} t_k^- = \sum_l n_{al} t_l^+ + n_a^+ \quad (4)$$

148 holds for all atom types a and, likewise, the charges satisfy

$$q^- + \sum_k t_k^- q_k^- = \sum_l t_l^+ q_l^+ + q^+ \quad (5)$$

149 The practical complication is that (i) the set of possible compounds that may appear
150 as additional reactants or products is too large for brute force enumeration, and (ii)
151 even if this were possible, not all choices that formally might solve the problem are
152 chemically plausible. To simplify the notation further, we can treat the charge as an
153 additional formal “atom type” that may take on both positive and negative integer
154 values, corresponding to positive and negative charges, respectively. This amounts to
155 considering free electrons e^- as a special compound. Moreover, we write n_q^- and n_q^+
156 instead of q^- and q^+ for the net charge in the following. Note that by convention a
157 free electron e^- corresponds to a charge of -1 . In the remainder of this section, we
158 describe two alternative strategies for rebalancing chemical reactions.

159 2.2 Rule-based Method

160 2.2.1 Representation of Molecules and Reactions

161 It is common well-known issue that entries in reaction databases often omit one or
162 more simple compounds such as H_2O , NH_3 , and HCl .

163 To rebalance such incomplete reaction data, we developed a specialized rule library
164 to systematically incorporate these missing elements utilizing the cheminformatics
165 library `RDKit 2023.9.4` [44]. To facilitate computations, we represent the sum formula
166 of molecules as a dictionary.

$$\mathcal{D} := \{C_1 : n_1, C_2 : n_2, \dots, C_\ell : n_\ell, Q : n_Q\}$$

167 Here, each C_a , $1 \leq a \leq \ell$, is an atomic symbol, i.e., H, O, or N, and $n_a \in \mathbb{N}$ is the
168 number of atoms of type C_a in the compound under consideration. We use the special
169 symbol Q to denote charge associated with the molecule. Recall that $n_Q \in \mathbb{Z}$ can be
170 positive, negative, or zero.

171 The rule-based strategy is applied only to reactions that are carbon-balanced. The
172 reason is that in organic reactions, the structure of the carbon backbone plays a key
173 role, and thus, sum formulas are much less likely to be sufficient to completely describe
174 the missing molecules. We also optimized our approach by considering the standard
175 representation of ions in chemical equations, such as OH^- and H^+ , instead of $NaOH$
176 or HCl . To achieve this, we restructured our rule library to focus on elementary ions,
177 enabling us to interpret compounds such as HCl in terms of their constituent ions, H^+
178 and Cl^- . This refinement led to a more efficient and compact rule library, as depicted
179 in Table S3.

180 We denote by \mathcal{D}^- and \mathcal{D}^+ the composition dictionaries of the sum of the molecular
181 formulae of reactants and products, respectively. That is, \mathcal{D}^- has entries of the form

182 $C_a : n_a^-$, and \mathcal{D}^+ has entries $C_a : n_a^+$. The discrepancy between \mathcal{D}^- and \mathcal{D}^+ is
183 conveniently represented by two dictionaries Δ^+ with entries $C_a : n_a^+ - n_a^-$ provided
184 $n_a^+ > n_a^-$, and Δ^- with entries $C_a : n_a^- - n_a^+$ provided $n_a^+ < n_a^-$. Thus Δ^+ accounts for
185 the atoms only present in the products and Δ^- accounts for the atoms only present
186 in the reactants.

187 Based on the difference dictionaries Δ^\pm we distinguish four cases:

- 188 - *balanced* if $\Delta^+ = \Delta^- = \emptyset$,
- 189 - *reactant-dominated* if $\Delta^- \neq \emptyset$ and $\Delta^+ = \emptyset$,
- 190 - *product-dominated* if $\Delta^+ \neq \emptyset$ and $\Delta^- = \emptyset$,
- 191 - *both-sides* if both $\Delta^- \neq \emptyset$ and $\Delta^+ \neq \emptyset$.

192 If only one of Δ^- and Δ^+ has a non-charge entry, then the charge difference is
193 accounted for in the same dictionary, while the other one is left empty. This is always
194 possible since charges may be positive or negative. Instances of the both-sides case,
195 i.e., instances with missing atoms in both reactants and products are not considered
196 further here. They require a more sophisticated approach and are relegated to the
197 MCS-based method in our current implementation.

198 Reactant-dominated and product-dominated cases are handled in the same man-
199 ner. In the following, we denote by Δ the single non-empty difference dictionary.

200 For example, the database entry

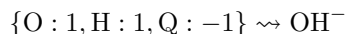


201 yields the dictionaries $\mathcal{D}^- = \{\text{C} : 4, \text{H} : 10, \text{O} : 3\}$ and $\mathcal{D}^+ = \{\text{C} : 4, \text{H} : 8, \text{O} : 2\}$ for
202 the reactants and product, respectively, and thus $\Delta^- = \{\text{O} : 1, \text{H} : 2\}$.

203 2.2.2 Molecular Imputation

204 For ease of presentation we assume $\Delta = \Delta^-$, i.e., atoms are missing on the product
205 side only. Otherwise, the role of reactants and products is interchanged.

206 We consider a set \mathcal{R} of rules that explain (part of) the dictionary Δ in terms of
207 molecules X_k that are added to the product side. Our goal is to find a sequence of rule
208 applications which stepwise reduce the difference dictionary Δ and collect a multiset
209 S of molecules. Each $r \in \mathcal{R}$ is of the form $\hat{r} \rightsquigarrow X_r$, where \hat{r} is a dictionary and X_r
210 is a corresponding molecule. The application of a rule changes Δ accordingly. Since our
211 rules make use of simple ions, we allow arbitrary changes of charges. The rule



212 applies to dictionary $\Delta = \{\text{O} : 1, \text{H} : 2\}$ by adding OH^- to the products and updating
213 the dictionary to $\Delta = \{\text{H} : 1, \text{Q} : 1\}$. The resulting reaction is still unbalanced and
214 reactant-dominated, hence another rule may apply.

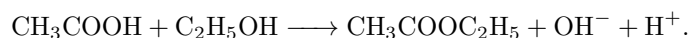
215 If we reach $\Delta = \emptyset$, then adding S to the products balances the reaction. In practice,
216 this can be achieved by the basic DFS search [45] outlined in Alg. 1. A call to $\text{DFS}(\Delta,$
217 $\mathcal{R}, \emptyset)$ either returns all (multi)sets of compounds S that balances the reaction and
218 leaves an empty dictionary Δ , or it terminates without output. By $\Delta \ominus \hat{r}$ we denote
219 the dictionary Δ after being modified by the application of a rule r .

Algorithm 1 DFS-like rule application

```
1: function DFS( $\Delta$ ,  $\mathcal{R}$ ,  $S$ )
2:   if  $\Delta = \emptyset$  then
3:     Yield  $S$ 
4:   else
5:     for each rule  $(\hat{r} \rightsquigarrow X_r) \in \mathcal{R}$  applicable to  $\Delta$  do
6:        $\Delta' \leftarrow \Delta \ominus \hat{r}$     $S' \leftarrow S \cup \{X_r\}$ 
7:       DFS( $\Delta'$ ,  $\mathcal{R}$ ,  $S'$ )
8:     end for
9:   end if
10: end function
```

220 The DFS algorithm yields all balancing solutions. These are passed on to the post-
221 processing step (2.2.3). The list \mathcal{R} of rules is applied in a fixed order that ensures
222 that pattern size, defined as the number atoms in \hat{r} , is non-increasing. Thus, the
223 search can be restricted to check only patterns with a valid length. One could use
224 the fact that the dictionary obtained by the successful application of several rules is
225 independent of the order in which these rules are applied. Keep track of the rule r that
226 was applied before DFS(Δ , \mathcal{R} , S) was called it therefore suffices to disregard in the
227 next recursion step all rules that appear before r in \mathcal{R} . Moreover, one could abandon a
228 recursion step if its path length exceeds the best previously found solution. The latter
229 modification however limits the scope of post-processing rules intended to remove
230 chemically implausible solutions. Since simple DFS is already comparably fast and the
231 search tree is usually quite shallow, such optimizations are currently not implemented.

232 Continuing the example, after the first match, we may apply the rule $\{\text{H} : 1, \text{Q} :$
233 $1\} \rightsquigarrow \text{H}^+$, which leaves the dictionary Δ empty. The DFS function first gives $S =$
234 $\{\text{OH}^-, \text{H}^+\}$ and we arrive at the (chemically correct) balanced reaction



235 In general, there will be multiple solutions. Thus, continuing the DFS after it yields
236 the first result turns it into an exhaustive search. The advantage of listing all solutions
237 is that they can be evaluated, and an optimal solution can be identified. Here, we use
238 the minimal number of rules as an optimization criterion. This favors matches of large
239 partial dictionaries. When multiple solutions exhibit an equivalent minimal count of
240 rules ascertained through the DFS algorithm, precedence is accorded to the solution
241 that encompasses an ion in the set S .

242 2.2.3 Post-processing

243 In some cases, the balancing of a reaction using DFS(Δ , \mathcal{R} , \emptyset) yields a formally
244 correct solution that is chemically implausible. More precisely, S may contain one or
245 more molecules that are at least unlikely to be the true reactants or products. In
246 some cases, it is possible to find a more plausible rebalancing. Oxygen and halogens
247 are typically formed via potent oxidizing agents. Hydrogen, on the other hand, is

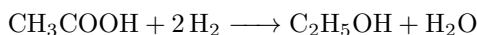
248 usually produced in reactions with alkali metals (e.g., lithium, sodium, potassium)
249 or hydride compounds. Whether this is the case can be checked after $\text{DFS}(\Delta, \mathcal{R}, \emptyset)$
250 has successfully balanced the reaction. Currently, SynRBL considers only three post-
251 processing rules:

- 252 (i) If a free halogen appears as a product, we assume that the solution is invalid and
253 reject the completion.
- 254 (ii) If oxygen O appears as a product, we add H_2 as a missing reactant and replace
255 O by H_2O on the product side.
- 256 (iii) If hydrogen H_2 appears on the product side and there is neither an alkali metal
257 nor a hydride among the reactant, we add O to the reactants and replace H_2 by
258 H_2O on the product side.

259 The software is designed in a manner that makes it straightforward to extend this rule
260 set.

261 2.2.4 Redox Reaction Refinement

262 Consider the reduction reaction involving the transformation of acetic acid into
263 ethanol: $\text{CH}_3\text{COOH} \longrightarrow \text{C}_2\text{H}_5\text{OH}$. The rule-based methodology aptly addressed this
264 reaction by introducing two moles of hydrogen H_2 to the reactant side and one mole
265 of water (H_2O) to the product side, thereby yielding the stoichiometric equation:



266 It is essential to acknowledge that the depicted reaction is not viable due to the insuffi-
267 cient reactivity of molecular hydrogen (H_2) for the reduction of acetic acid. Typically,
268 this reaction necessitates a suitable reducing agent, such as lithium aluminum hydride
269 (LiAlH_4). However, identifying and substituting the appropriate reducing agents can
270 be problematic. Some chemists use a convention to simplify chemical notations where
271 the reducing agent is represented as [H] without specifying the exact compound. Fol-
272 lowing this convention, we have updated the notation from molecular hydrogen (H_2)
273 to two single hydrogen atoms (H). This new representation indicates the presence of a
274 reducing agent distinct from elemental hydrogen. Likewise, the depiction of molecular
275 oxygen as O_2 has been revised to two single oxygen atoms (O), symbolizing its role
276 as an oxidizing agent.

277 2.3 MCS-based method

278 2.3.1 Determination of Missing Carbon Compounds

279 Carbon-unbalanced reactions cannot be meaningfully handled at the level of sum
280 formulas. Instead, it is necessary to make use of the structures of reactant and product
281 molecules. To this end, we represent both the reactants and the products of a reaction
282 as graphs whose connected components are the molecules. In these graphs, vertices
283 are labeled by atom types and edges correspond to chemical bonds, annotated by
284 their bond type. Since reactions with carbon atoms missing on the reactant side are
285 treated in the same way as reactions with missing carbon on the product side, we fix
286 the notation as follows:

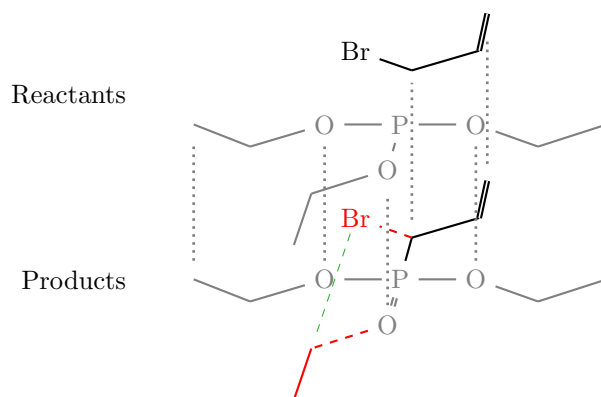


Fig. 1: In this example two fragments (shown in red) remain unmatched: Br with a single bond as cut, and an ethyl group also with a single bond. The cut edges of the fragments are show as dashed red lines. A merge rule insert a single bond (dashed green) connecting the end-points of the cut edges.

287 Let X and Y be the graphs with the larger and smaller number of carbons, respec-
 288 tively. Moreover, we write $\mathcal{X} = \{X_1, X_2, \dots, X_k\}$ for the set of connected components
 289 of X . Assuming that all missing carbons belong to one connected compound Y_* miss-
 290 ing on the Y -side of the reaction, we can conclude that Y_* is in essence a part of some
 291 X_i . In order to identify this part, we compute, for each $X_i \in \mathcal{X}$, a maximum *con-*
 292 *nected* common subgraph $M_i = \text{MCS}(X_i, Y)$. There are several choices for the exact
 293 definition of the function $\text{MCS}(\cdot)$, which we will discuss in more detail below. For
 294 the moment we only require that the subgraph M_i is connected and that $\text{MCS}(\cdot)$
 295 defines an injective map of the vertex set $V(M_i)$ into $V(X_i)$ and $V(Y)$ where each
 296 vertex in $V(Y)$ is only mapped once. We can therefore identify the vertices of M_i
 297 with a subset of the vertices of X_i and, by a slight abuse of notation, simply write
 298 $V(M_i) \subseteq V(X_i)$. This, in turn, specifies a (bipartite) matching between vertices of X_i
 299 and Y that correspond to the same vertex of M_i . In chemical terms, this matching is a
 300 partial atom-atom map between X_i any Y and thus also between X and Y . To charac-
 301 terize the part of X_i that does not match Y in more detail, we consider the subgraph
 302 $A_i := X_i[V(X_i) \setminus V(M_i)]$ of X_i induced by the unmatched vertices. Moreover, let B_i
 303 be the edge cut between $V(A_i)$ and $V(M_i)$ in X_i . In chemical terms, B_i denotes the
 304 bonds that separate M_i and A_i and thus were broken (or formed) by the reaction. A
 305 vertex in A_i is said to be a *boundary vertex* if it is incident to a cut edge $e \in B_i$.

306 Denote by $\mathcal{A} := \{(A_i, B_i) | X_i \in \mathcal{X}\}$ the set of auxiliary graphs together with their
 307 separating edge cuts. We shall refer to these as *fragments*. By construction, \mathcal{A} contains
 308 the relevant information on the mission compounds because the union $\bigcup_i V(A_i)$ is the
 309 set of missing atoms, and the B_i are bonds on X_i that are broken in order to obtain
 310 Y . The task at hand, therefore, is to “recombine” the (A_i, B_i) in a way that recovers
 311 the missing compound(s) Y_* . To this end, we again pursue a rule-based approach. We
 312 consider two types of rules:

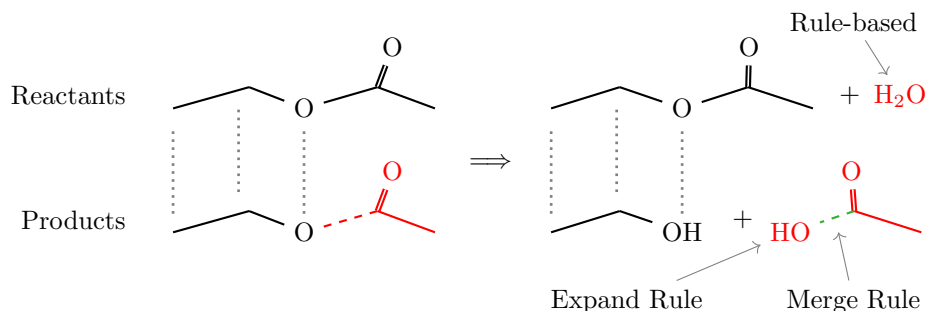


Fig. 2: Graph alignment and imputation of missing parts (red). The absence of the second reactant is solved by applying an *expand rule* before merging the fragments with an appropriate *merge rule*.

313 **Merge rules** encode conditions for the insertion of edges between two boundary ver-
 314 tices, $u \in V(A_i)$ and $v \in V(A_j)$ located in distinct fragments, see Fig. 1. These rules
 315 depend on the specific boundary configuration, i.e., the chemical context of the two
 316 boundary atoms u and v . The application of a merge rule not only inserts a bond
 317 (labeled edge) between u and v , but also removes the respective cut edges incident to
 318 u and v from B_i and B_j , respectively. Thus only one merge rule is applied for each
 319 boundary. The boundaries are then considered resolved in the chemical domain. More-
 320 over, open boundaries on the same compound are never merged with each other. Hence,
 321 this step always needs at least two compounds. If only one is available, *expand rules*
 322 are applied first to add the missing second fragment. A collection of merge rules is pro-
 323 vided as configuration file and can easily be extended or modified in SynBRL. Table S1
 324 in the supplementary lists the currently implemented merge rules. The alignment and
 325 imputation on a simple example are depicted in Fig. 1.

326 **Expand rules** are used to add nodes to the molecular graph based on the boundary
 327 configuration of unmatched fragments. More precisely, they can add fragments with
 328 boundaries to \mathcal{A} depending on what is needed for unresolvable cut edges. This is in
 329 particular the case if \mathcal{A} comprises only a single fragment (A, B) . The idea of the expand
 330 rules is to add additional atoms such that cut edges that do not have a counterpart in
 331 another fragment are “saturated”. Technically, however, an *expand rule* only adds the
 332 required atom, and the actual bond is then formed by a *merge rule*. Expand rules are
 333 also specified in a configuration file. Table S2 in the supplementary lists the currently
 334 implemented merge rules.

335 Each application of a merge step reduces the number of cut edges in the fragment
 336 set \mathcal{A} . Repeated rule application either terminates prematurely with no further appli-
 337 cable rule, or it succeeds replacing all cut-edges, thus resulting in a graph Z without
 338 remaining boundary vertices. By construction, the reaction $X \rightarrow Y \cup Z$ is now car-
 339 bon balanced. It is not balanced in general. Note that the expand steps have added
 340 additional non-carbon atoms.

341 In practice, most carbon unbalanced reactions are missing a structure at the
 342 product side of the reaction. Hence, the methodology focuses on reactant-dominant

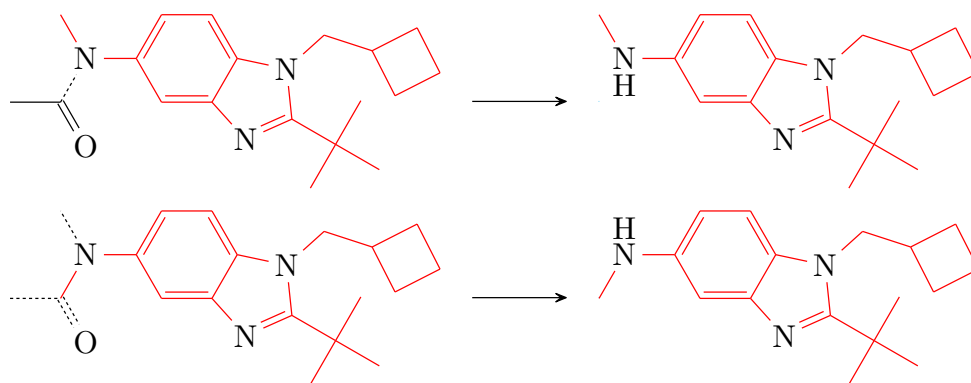


Fig. 3: Example of the ambiguity of the MCS. The product has two distinct isomorphisms in the reactant. The first example has one resulting fragment, and the second has three fragments. Dotted lines indicate the broken bonds.

343 reactions. In principle, it can be applied to product-dominant reactions as well. How-
 344 ever, imputing a missing reactant is more challenging than finding a missing product.
 345 A single reaction equation can often contain multiple reaction steps, leading to mul-
 346 tiple equally correct intermediate compounds that could be added to the reactants to
 347 form a balanced reaction. Since these cases are of minor practical relevance, we have
 348 no attempted to formulate specific rules for product-dominant reactions.

349 Fig. 2 shows a simple de-esterification as an example. Here, only one missing frag-
 350 ment is detected. Because the carbon-oxygen bond is part of an ester group, an expand
 351 rule adds the missing oxygen atom to the reaction. In the second step, a merge rule
 352 connects this oxygen with a single bond to the open boundary on the identified frag-
 353 ment, creating the missing acetic acid. The resulting reactions is carbon balanced but
 354 unbalanced overall. The rule-based method described in Section 2.2 is now applicable
 355 to add the missing water molecule to the reactants.

356 2.3.2 Computing Maximum Common Molecular Subgraphs

357 Maximum common subgraph (MCS) problems come in different variants. Both the
 358 maximum common induced subgraph (MCIS) problem and the maximum common
 359 edge subgraph (MCES) problem, as well as their restrictions to connected common
 360 subgraphs, are NP-hard [40]. Nevertheless they can be solved efficiently for small pairs,
 361 and thus also for molecules. However, none of the variants of combinatorial optimiza-
 362 tion problem is guaranteed to identify the “chemically correct” common subgraph,
 363 i.e., the one that correctly identifies all bonds that change during a chemical reaction.

364 While the size of an MCS is uniquely defined, neither the common subgraph nor
 365 its embedding is unique in general. In the example in Fig. 3 the subgraph isomorphism
 366 for the red subgraph is not unique. This is a well-known issue for the construction
 367 of atom-atom-mapping tools. These ambiguities are not easily resolved because the
 368 combinatorial MCS problems operate on graphs rather than a more detailed model of
 369 the molecules that encompasses also e.g. hybridization or partial charges.

370 In order to improve over the application of any one particular problem variant
 371 or algorithm, SynRBL resorts to the heuristics implemented in RDKit [44] and com-
 372 putes several alternative variants: MCIS is addressed using the Fragment Matching and
 373 Compound Similarity (FMCS) [46], while the Rascal algorithm [47], as implemented
 374 in the RDKit library, is used to solve the MCEs problem. Moreover, an ensemble
 375 method that amalgamates outcomes from five distinct configurations, detailed in
 376 Table 1 is used. Each of these specifies additional constraints on the matches allowed
 377 in the corresponding MCIS or MCEs variant. Both the `RingMatchesRingOnly` and
 378 the `CompleteRingsOnly` ensure that atoms in rings match atoms in rings only. In
 379 graph-theoretical terms this corresponds to singling out the vertices in non-trivial 2-
 380 connected components. With the latter option, rings must be matched completely. In
 381 addition, bond order (treated as edge label) can be used as a constraint to prohibit
 382 the matching on single and double bonds.

Table 1: MCS Configuration

Configuration	1	2	3	4	5
<code>RingMatchesRingOnly</code>	True	True	False	False	-
<code>CompleteRingsOnly</code>	True	True	False	False	-
<code>Ignore Bond Order</code>	True	False	True	False	-
Algorithm	FMCS	FMCS	FMCS	FMCS	RASCAL

383 In order to deal with alternative embeddings of the MCS, we enumerate all maximal
 384 solutions of $\text{MCS}(X_i, Y)$ and identify the solutions that minimize the number of frag-
 385 ments resulting from the removal of the common subgraph. In the example in Fig. 3,
 386 one isomorphism corresponds to the disruption of the amide bond CO-N, thereby
 387 producing one additional fragment. The alternative embedding of the same common
 388 subgraph implies breaking bonds containing the amine bond CH₃-N, resulting in
 389 three additional fragments. Hence, we choose the former embedding.

390 In order to keep the computational costs low, we do not compute $\text{MCS}(X, Y)$
 391 directly, but instead use an iterative approach that successively aligns the components
 392 $X_i \in \mathcal{X}$ and removes the matched vertices from Y . More precisely, for each $X_i \in \mathcal{X}$
 393 we compute $\text{MCS}(X_i, Y^{(i-1)})$ and construct $Y^{(i)}$ by removing all matched vertices from
 394 $Y^{(i-1)}$. To do this efficiently, we sort \mathcal{X} in order of decreasing number of vertices in the
 395 connected components. As part of each evaluation of $\text{MCS}(X_i, Y^{(i-1)})$ we also keep
 396 track of the cut edges between the matched and unmatched vertices, i.e., the broken
 397 bonds, which in particular allows us to compute the (A_i, B_i) from the iterative MCS
 398 approach.

399 2.4 Interaction of the two Methods

400 The rule-based method offers efficient solutions for non-carbon compounds, whereas
 401 the MCS-based approach focuses on subgraphs to find missing carbon structures.
 402 Identifying the optimal common subgraph is computationally intensive, making the
 403 MCS-based method less suitable for non-carbon compounds. Consequently, applying
 404 the two methods complementarily, each to their respective optimal scenarios, enhances

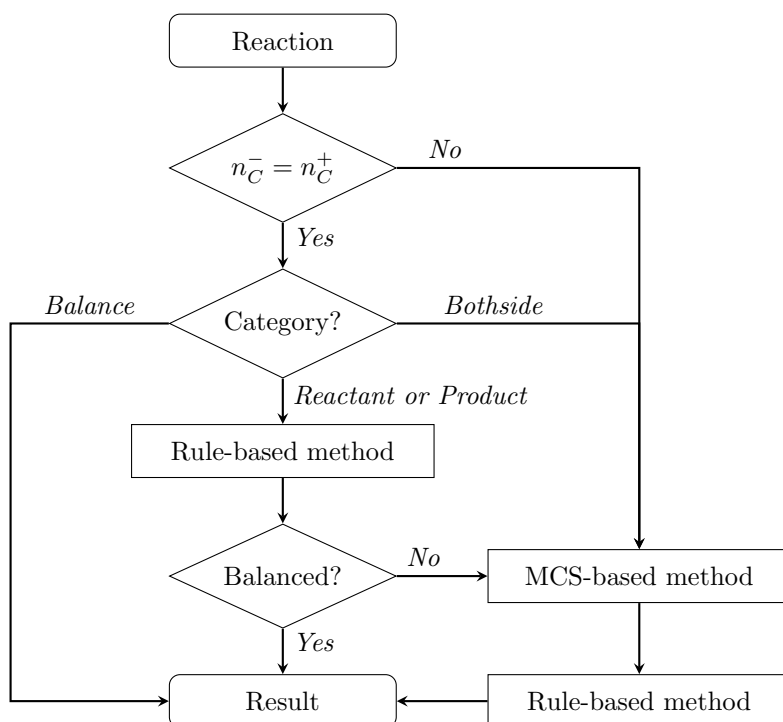


Fig. 4: Simplified overview of the functional process in **SynRBL**. The rule-based method is applied if the reaction is carbon-balanced but otherwise unbalanced in either the reactant or the product side. The MCS-based method is used if both sides are unbalanced, the rule-based method fails, or the reaction has a carbon imbalance in the first place. The output is either the balanced reaction if the method is successful or the unmodified input in case **SynRBL** can not find a solution.

405 overall efficiency: the rule-based approach for non-carbon compounds and the MCS-
 406 based method for situations where subgraph analysis is advantageous. The overall
 407 framework is summarized in Fig. 4. Reactions identified as *bothside* have a non-carbon
 408 imbalance on the reactant and product side. These cases are not solvable by the
 409 rule-based method and are hence subject to the MCS-based method. Both methods
 410 utilize functions from **RDKit** [44]. Either for parsing reaction SMILES or handling the
 411 molecular graph representation in the MCS-based method.

412 Just like the rule-based method, the MCS-based method can only solve some imbal-
 413 ances. More precisely, the approach depends on the identification of the chemically
 414 correct MCS. The method outlined above, in particular, cannot handle rearrange-
 415 ment reactions or ring-formations. We shall return to this point in more detail, see
 416 Section 3.2 below. The MCS-based method also tends to fail if too many compounds
 417 or boundaries are found, the number of boundaries does not match, or the reaction is
 418 not carbon balanced afterwards, e.g., because not all carbon atoms in *Y* are covered

419 by MCS matches. On the other hand, if a solution is found, the confidence is high that
420 the result is in fact correct.

421 2.5 Datasets and Benchmarking

422 **SynRBL** is not trained on any specific dataset but leverages basic chemical knowledge
423 to inform its rule set. In order to assess its performance we use three widely used
424 public data collections: (i) an open-access tailored for CASP that incorporates the
425 **Golden** dataset [27], (ii) Jaworski’s dataset [19], and (iii) the **USPTO_50k** collection [5].
426 The latter contains more than 50,000 reactions. We extracted a representative sub-
427 set comprising only unbalanced reactions and selected validation datasets based on
428 three different strategies, resulting in the following three datasets. The *USPTO Random Class*
429 dataset (**Urnd**) was chosen utilizing a stratified sampling method across ten
430 varied chemical reaction classes. Additionally, the *USPTO Different* dataset (**Udiff**)
431 was selected employing a similar stratified strategy, albeit with Δ , the difference in
432 the dictionaries representing reactants and products, to ensure a comprehensive rep-
433 resentation of the diversity in molecular formulas between reactants and products.
434 The *USPTO Unbalance Class* (**Uunb**) was selected by randomly choosing from reac-
435 tions classified as solved or unsolved by the rule-based method. This selection provides
436 insights into carbon and non-carbon imbalances within the chosen reaction classes. To
437 ensure reproducibility, the random seed was set to a fixed value (seed value = 42) for
438 all random selection processes. The datasets are summarized in Table 2.

Table 2: Composition of validation datasets in different categories

Dataset	Reactions	C _{unb}	Balance	Unbalance
Golden	1851	729	209	913
Jaworski	637	116	302	219
Urnd	803	328	0	475
Udiff	1589	355	0	1234
Uunb	540	257	0	283
Total	5420	1785	511	3124

439 In order to benchmark **SynRBL** we evaluated (1) *success* of the algorithm, defined as
440 the fraction of (unbalanced) instances for which **SynRBL** proposed a balanced reaction,
441 and (2) *accuracy*, the fraction of proposed solutions for the rebalancing problem that
442 are (chemically) correct.

443 2.6 Estimating Prediction Confidence

444 The results for the five datasets mentioned in Table 2 were checked manually by
445 TLP, the first author, an experienced chemist. We reviewed all reactions to determine
446 their chemical validity, typically focusing on whether the reaction center or bond
447 changes were valid. The results presented in Section 3 provide a good indicator of how
448 many of the imputations should be correct. However, validating individual outcomes
449 necessitates the expertise of a domain specialist. Predicting a confidence for results

450 from the MCS-based method can be used to filter out potentially wrong imputations
451 and increase the accuracy of the method. We observed that the accuracy strongly
452 depends on the complexity of the reaction center, for example on the number of bonds
453 involved in the reaction. We therefore developed a machine learning model using the
454 XGBoost algorithm [48] (version 2.0.3) to predict a confidence value for our imputations
455 based on the reaction properties illustrated in Table 3. This model was trained on
456 80% of the 2275 reactions from the five datasets that are subject to the MCS-based
457 method, and the remaining 20% (455) of reactions are used for testing.

Table 3: Features for analysis.

Features	Description
<i>total_carbons</i>	The total count of carbon atoms present in the reactions.
<i>total_bonds</i>	The aggregate number of chemical bonds in the reactions.
<i>total_rings</i>	The total count of ring structures within the reactions.
<i>fragment_count</i>	The total number of distinct fragments or molecules present in the reactions.
<i>carbon_difference</i>	The discrepancy in the number of carbon atoms between reactants and products.
<i>num_boundary</i>	The count of boundary atom (reaction center) identified by MCS-based method.
<i>Bond Changes</i>	The maximum count of bonds formed in products or broken in reactants, a feature that requires manual extraction.
<i>bond_change_merge</i>	The net change in the number of bonds between reactants and products post-MCS process.
<i>ring_change_merge</i>	The net change in the number of rings between reactants and products post-MCS process.

458 To optimize the performance of the model in light of the imbalanced dataset,
459 where the number of correct and incorrect solutions varies significantly, we employ
460 the SMOTETomek algorithm [49] from imblearn 0.12.0 [50]. This technique combines
461 the Synthetic Minority Over-sampling Technique (SMOTE) with Tomek links to
462 effectively balance the dataset, thereby enhancing the predictive accuracy of our
463 model.

464 3 Results and Discussion

465 3.1 Rule-based Method

466 The rule-based approach of Section 2.2 is applicable on the reactions with missing
467 compounds among either the reactants or the products, with the stipulation that the
468 carbon must be balanced. This method yields a good *success* rate ranging from 89.60%
469 to 99.69% on our five benchmarking sets. It reaches a rather remarkable accuracy level
470 of up to 99.91% on the successful instances. These results are summarized in Fig. 6A
471 below.

472 *Analysis of Incorrect Predictions*

473 A careful inspection of invalid imputations revealed some systematic problems associ-
474 ated with specific datasets. Applied to data derived from the USPTO database (Urnd,

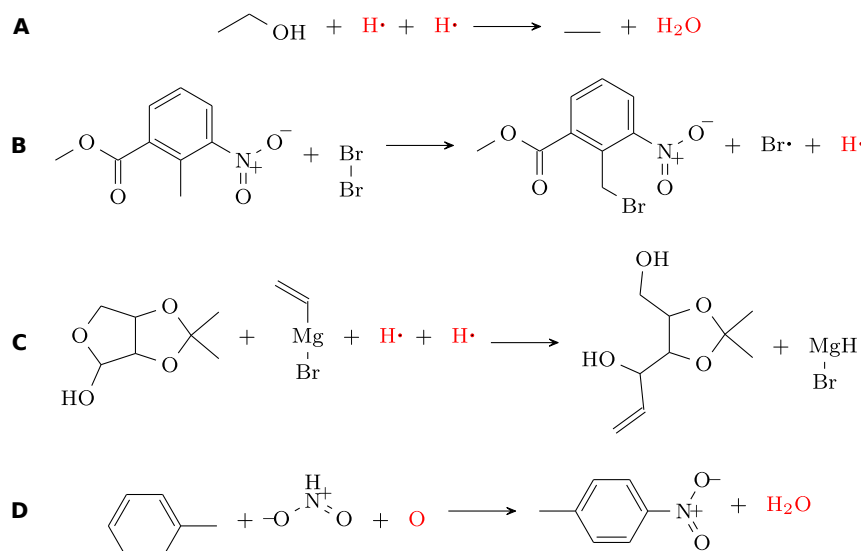


Fig. 5: Examples for incorrect imputations with the rule-based method. Original database entries are shown in black, imputed compounds in red. (A) An erroneous reaction from USPTO, with $\Delta = \{O : 1, Q : 0\}$, representing a sequence of dehydration and reduction reactions. (B) A correctly rebalanced reaction from Jaworski dataset that remains uncertain due to the presence of Hydrogen on the product side. (C) False imputation in Jaworski dataset where the product is mistakenly standardized as RMgH instead of RMg^+ . (D) An error in the rebalanced reaction in Golden dataset, due to HNO_2 being incorrectly identified instead of HNO_3 on the reactant side.

475 **Udiff, Uunb**) the rule base method produced uncertain predictions associated when
 476 $\{O : 1, Q : 0\}$ being on the reactant side during rule application. Consider, for exam-
 477 ple the conversion of ethanol to ethane in Fig. 5A, which is usually performed by
 478 dehydration and subsequent hydrogenation or by application of hydroiodic acid HI.

479 In the Jaworski dataset, two reactions were flagged as uncertain or invalid. The
 480 first instance involved the presence of hydrogen in the product without alkali met-
 481 als or hydrides. This anomaly was traced back to a precursor reaction involving a
 482 bromine radical $\text{Br}\cdot$, from which the the generation of a hydrogen radical $\text{H}\cdot$ is incor-
 483 rectly inferred. Instead of separate radicals, the formation of hydrogen bromide HBr
 484 is expected, see Fig. 5B. Further scrutiny revealed inaccuracies e.g. in Grignard Reac-
 485 tions, where the product was incorrectly identified as RMgH instead of RMg^+ . This
 486 error could be attributed to the standardized procedures of the original database,
 487 which led to the improper imputation of hydrogen on the reactant side. The approp-
 488 ropriate correction would be the addition of H^+ to the reactant side and RMg^+ to the
 489 product side, Fig. 5C.

490 In the Golden dataset we found 22 reactions with ambiguous status due to invalid
 491 reactants. Notably, the formation of nitrobenzene from benzene (id.481, Fig. 5D),
 492 erroneously specified nitrous acid HNO_2 instead of nitric acid HNO_3 as the reagent.

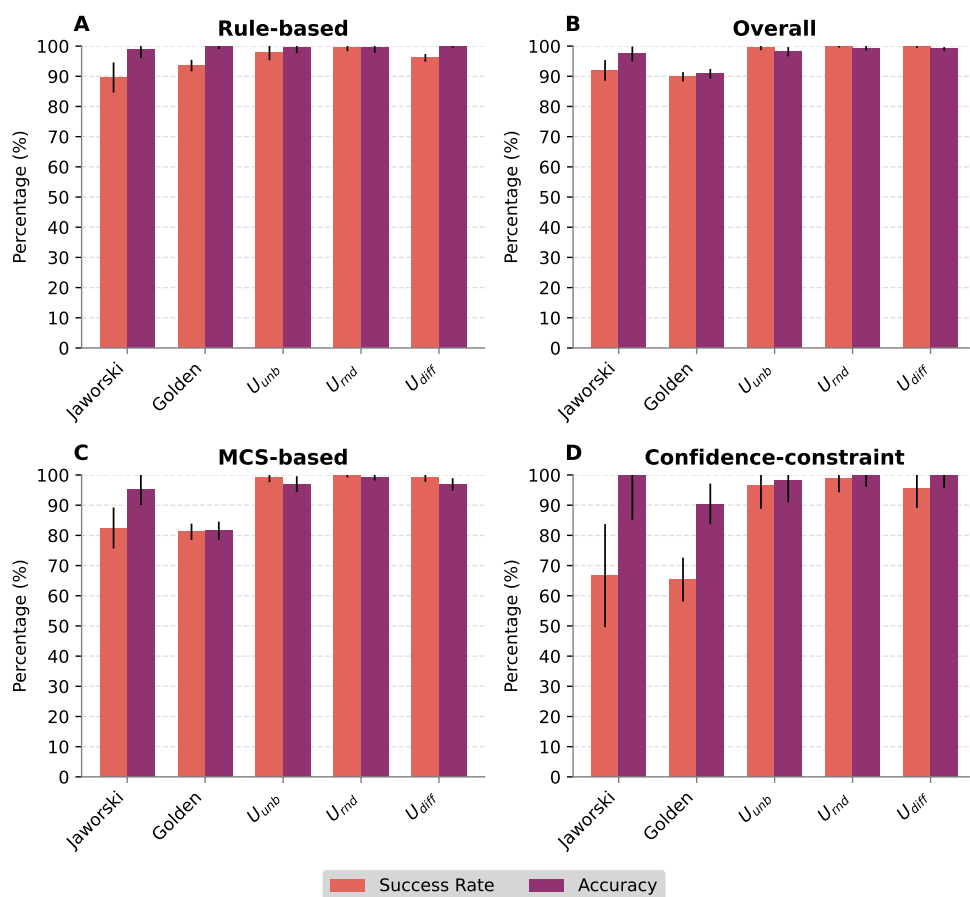


Fig. 6: Validation results for the rule-based method (A), the entire framework (B), MCS-based method (C), and the MCS-based method with an applied confidence threshold of 50% (D). Comparing (C) and (D) shows the tradeoff in success rate for higher accuracy when thresholding the predicted confidence. Because validation was only done on data that was not used in training (20% of the data), (D) has noticeably larger uncertainty margins.

493 The invalid reactions are enumerated in a dedicated supplementary file. A recurrent
 494 pattern observed in these reactions is that the rule-based method infers a singular
 495 oxygen O to be added to the reactant side.

496 Overall, however, the rule-based method rarely produces chemically incorrect or
 497 questionable imputations, at least when reactants and products are chemically accu-
 498 rate. The presence of isolated O or H in the prediction, on the other hand, appears to
 499 serve as an indicator for errors in the database entry.

500 The rule-based approach is challenging with respect to computational cost if
 501 the compounds contain a larger number of carbon atoms and, in particular, if the

502 number of carbon isomers becomes large. We also note that the method has diffi-
503 culties with carbon-imbalanced compounds in general. For example, in the reaction
504 $\text{CH}_3\text{COOC}_2\text{H}_5 \longrightarrow \text{CH}_3\text{COOH}$, a naive solution might suggest adding ethylene C_2H_4
505 to balance the product side. The correct solution, however, is to add water H_2O to the
506 reactants and ethanol $\text{C}_2\text{H}_5\text{OH}$ to the products. Since such examples are abundant,
507 we do not apply the rule-based method to carbon-imbalanced reactions.

508 3.2 MCS-based Method

509 The MCS-based method succeeds in 81% (**Golden** dataset) to 100% (**Urnd**) of the test
510 cases, see Fig. 6C and Supplementary Table S4. Fig. 7 depicts some reactions that
511 were successfully balanced by the MCS-based method. It showcases the application of
512 a list of different expand and merge rules. In contrast to the rule-based approach, the
513 prediction accuracy on successful cases is not fully satisfactory on all test sets. While
514 the predictions are close to perfect on the USPTO-based datasets, and about 95% for
515 the Jaworski’s data, only about 80% are achieved on the **Golden** set. The differences
516 in success rates between the datasets can be attributed primarily to differences in
517 the frequency of reactions that cannot be balanced by the MCS-based approach, in
518 particular rearrangement reactions, ring-formations, or complex reactions with many
519 compounds.

520 *Analysis of Incorrect Predictions*

521 Incorrect predictions arise in particular for complex reactions, and especially with
522 multi-step reactions. Fig. 8 illustrated examples of a ring-forming reaction and a rear-
523 rangement reaction where the MCS-based approach fails to identify a valid solution.
524 The structure highlighted as the MCS search result, particularly in Fig. 8B, exhibits
525 four boundaries, indicating an erroneous outcome from the MCS-based method.
526 Such reactions, not amendable by this method, are left unbalanced and represent a
527 limitation of our approach in its current form.

528 In order to better understand other factors contributing to incorrect predictions,
529 we investigated the influence of different features on the accuracy—see also Section 2.6.
530 Not surprisingly, the accuracy decreases with indicators for the “complexity” of the
531 reaction, particularly with the inferred number of broken/formed bonds, the total
532 number of substances in the reaction, and the number of boundaries. A similar trend is
533 found for the number of different bonds and cycles after graph merging. In contrast, the
534 performance does not depend systematically on the carbon imbalance $|n_{\text{C}}^+ - n_{\text{C}}^-|$. The
535 total number of compounds in a reaction exceeds 6 only in some entries in the **Golden**
536 dataset since it also reports catalysts and solvents. This suggests that the performance
537 declines with more fragments due to potential substance-matching misalignments. In
538 some cases, no boundaries were detected in the MCS step. The lack of accuracy in
539 the absence of a boundary strongly suggests to exit without success if no boundary is
540 found, since the result is almost always wrong anyway. The details of this exploratory
541 data analysis are summarized in Supplementary Fig. S2.

542 In order to understand the factors influencing accuracy in more detail we performed
543 a feature importance study summarized in Fig. 9A. The feature importance is the
544 average gain, i. e. the relative contribution of each feature for a given prediction over

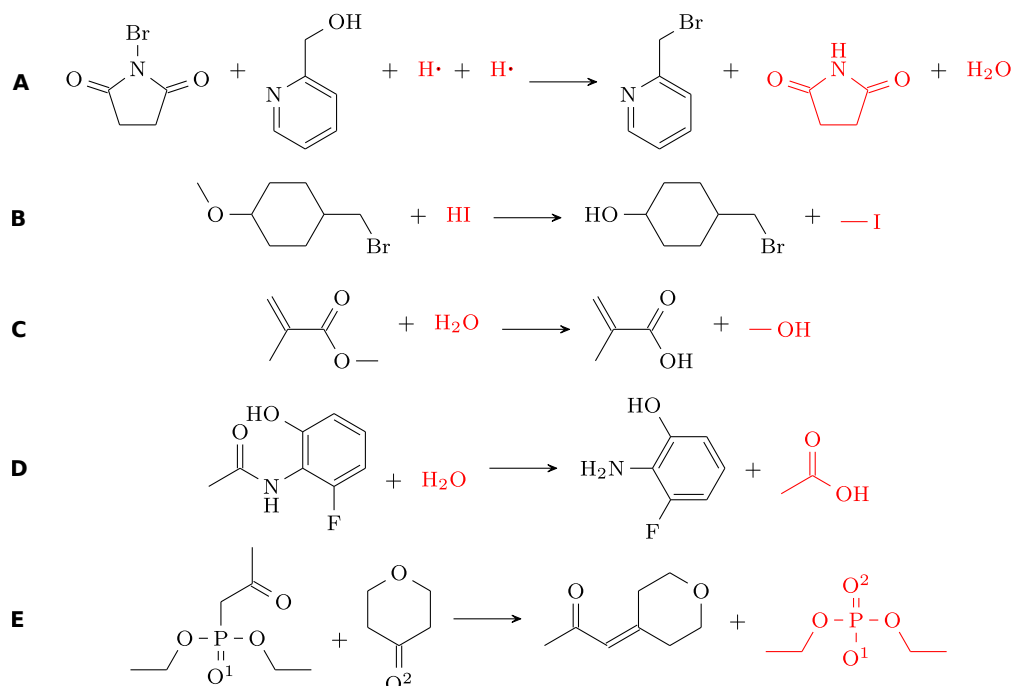


Fig. 7: Some examples of reactions solved by the MCS-based method showcasing different merge and expand rules. Data base entries are shown in black, imputed compounds in red. (A) Append compounds without forming a bond. (B) Append and merge I on Ether break. (C) Append and merge O on Ether break. (D) Append and merge O on Amide break. (E) Create new double bond with P. The double bond between O^1 and P in the reactant is changed to a single bond in the product and the oxygen O_2 from the oxan-4-one creates a double bond with P.

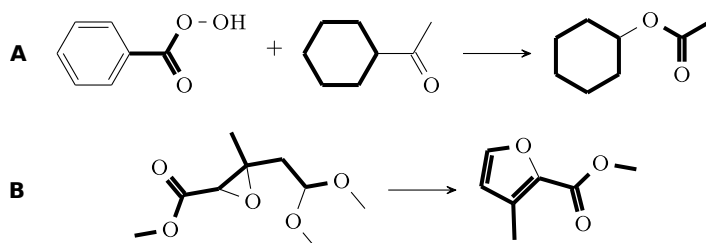


Fig. 8: Two examples that are not solvable by the MCS-based method. The MCS is not meaningful for these types of reactions. (A) Example for an unsolvable oxidation and rearrangement reaction. (B) Example for an unsolvable ring forming reaction. Bold lines indicate the identified MCS.

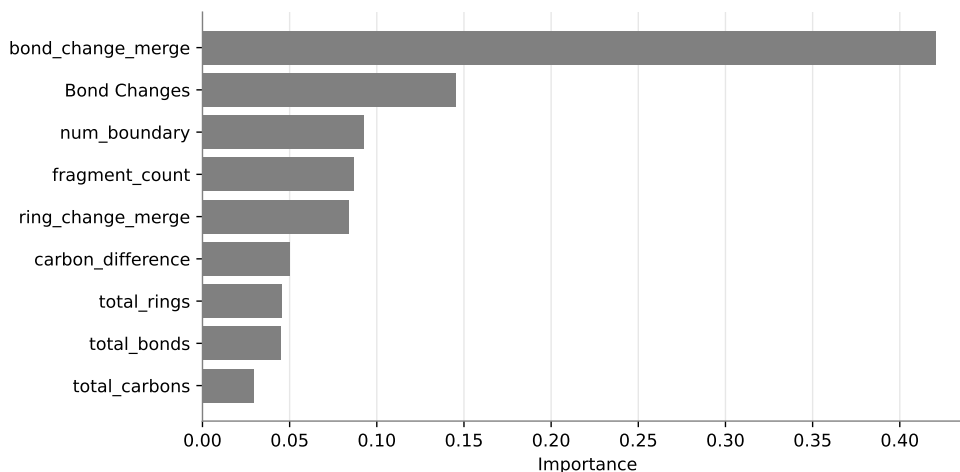


Fig. 9: Feature importance analysis provides a detailed visualization of various factors influencing the precision of the MCS-based method.

545 all targets. In line with the exploratory analysis described above, we observed that
 546 the total number of carbons, bonds, rings, and the difference in carbon content within
 547 the reaction does not significantly influence the performance of **SynRBL**. Surprisingly,
 548 the disparity in the bond count after graph merging emerged as the most impact
 549 factor, surpassing even the number of bond changes in predictive power. In order to
 550 investigate the interplay between the most informative factors, we also considered the
 551 co-occurrences of the number of different bonds after merging, the number of different
 552 rings after merging, the count of boundaries detected, and total number of compounds,
 553 see Fig. S3.

554 Taken together, this analysis establishes parameters for which we can expect reli-
 555 able rebalancing results: bond changes after merging should not exceed three; ring
 556 changes should be fewer than two; reaction not involve more than four molecules, and
 557 only one or two boundaries should be detected.

558 As a more quantitative approach, we devised a scoring function that summarizes
 559 the feature analysis and allows to estimate the confidence level of our predictions,
 560 see Section 2.6. The performance of our model is detailed in Supplemental Fig. S4,
 561 showcasing strong predictive capabilities with an F1-score (micro) of 0.92, an AUC of
 562 0.94, and an AP of 0.81. Using a confidence threshold of 50%, leads to the expected
 563 increase in accuracy of the MCS-based predictions for both Jaworski’s dataset and the
 564 **Golden** dataset, at a moderate decline in success rate, see Fig. 6D. This observation
 565 underscores the robustness of the method in enhancing prediction reliability through
 566 the strategic application of a confidence threshold.

3.3 Performance of the Combination of Rule-base and MCS-base Components

The interplay of the rule-based and MCS-based methods described in Section 2.4 results in a satisfactory performance of the SynRBL framework. Fig. 6C shows that the tool reaches success rates between 89.8% (Golden) and 100% (Urnd) at accuracies between 90.8% (Golden) to 99.4% (Urnd). More detailed values are listed in Supplementary Table S4. The significantly lower performance metrics observed within the Golden dataset can be attributed to the inherent complexity of its reactions, which also include the presence of solvents and catalysts. These elements introduced additional variables into the molecular alignment process, thus posing significant challenges to the predictive capabilities of this framework. In addition, we evaluated the computational efficiency of our methods, observing an average processing time of 46 seconds per 1000 reactions on an average workstation where one-third of the reactions were solved by MCS. In our comparative analysis, our method surpassed the current state-of-the-art, ChemMLM [29], demonstrating superior performance in both *success rate* and *accuracy*. The reported outcomes for ChemMLM showed a *success rate* fluctuating between 4.1% to 42.7% on the USPTO dataset. In contrast, SynRBL demonstrates a remarkable *success rate* of 99% or higher on the same dataset. Moreover, while the *accuracy* of ChemMLM varied widely (from 100% for shorter SMILES strings to a mere 8.2% for larger molecules), SynRBL's accuracy remains robust, largely unaffected by molecular size, and consistently exceeds 98% across the USPTO dataset.

4 Conclusion

In this contribution, we investigated the SynRBL framework as an innovative approach for the rebalance of incomplete reaction entries in chemical databases. SynRBL combines a rule-based approach for carbon-balanced reactions and the MCS-based workflow for carbon-unbalanced reactions. The latter combines variants of the MCIS and MCES problem to increase the fraction of instances in which chemically correct subgraph embedding is found. For the MCS-based component, moreover, a trained feature-based machine learning model was used to estimate the prediction confidence. SynRBL was rigorously evaluated based on five meticulously curated validation datasets, encompassing a subset of the Golden dataset, the Jaworski dataset, and three variants of the USPTO 50k database. Overall, the framework achieves unprecedented accuracy, exceeding 99% on the subset of database entries that it can process successfully. These cover more than 90% of the unbalanced reactions in the datasets used for evaluation. As a by-product of the rule-based analysis, we observed that the signature $O : 1, Q : 0$ referring to a single oxygen is as a strong indication for an error in database entry.

The current implementation of SynRBL is limited to product-dominated or reactant-dominant reaction entries. Moreover, it does not cover certain types of carbon-unbalanced reactions, in particular cyclizations and other complex rearrangement reactions that are difficult for the MCS-based branch of the framework. The SynRBL software is designed, however, to facilitate future extensions of the rule sets as well as of the MCS strategies. SynRBL is not based on a machine learning approach.

610 Instead, it makes use of “textbook-level” knowledge of chemical reactions in combi-
611 nation with conceptually simple optimization problems. While it does not cover all
612 situations and hence leaves a few percent of the database entries unbalanced, this
613 approach has the advantage of being independent of specific training data and thus
614 of biases inherent in specific data sources. We observed that it indeed yields robust
615 results for datasets with very different chemical content.

616 Reaction rebalancing with **SynRBL** can provide much larger and more diverse sets
617 of stoichiometrically balanced reactions as a basis for a wide variety of data-driven
618 tasks in cheminformatics. In particular, we expect that better atom-atom-maps can
619 be obtained from such balanced data since the mappers are freed from the need
620 to solve the reaction balancing problem simultaneously. We expect beneficial effects
621 also on learning approaches, e.g. in forward prediction, retrosynthesis planning, and,
622 notably, the elucidation of reaction mechanisms. Finally, representations of reaction
623 mechanisms in the form of graph transformation rules [51] could be employed as an
624 orthogonal validation strategy, particularly on data sources where *named reactions* are
625 annotated in the metadata.

626 5 Availability of Data and Materials

627 The datasets supporting the conclusions of this article are available in the **SynRBL**
628 repository: <https://github.com/TieuLongPhan/SynRBL/tree/main/Data>. The source
629 code is available at: <https://github.com/TieuLongPhan/SynRBL>.

630 6 Acknowledgement

631 This project has received funding from the European Union’s Horizon 2021 research
632 and innovation program under the Marie Skłodowska-Curie grant agreement No
633 101072930 (TACsy – Training Alliance for Computational systems chemistry).

634 References

- 635 [1] Lowe DM (2012) Extraction of chemical structures and reactions from the liter-
636 ature. Tech. rep., Apollo – University of Cambridge Repository, DOI 10.17863/
637 CAM.16293
- 638 [2] Goodman J (2009) Computer software review: Reaxys. Journal of Chemical
639 Information and Modeling 49(12):2897–2898, DOI 10.1021/ci900437n
- 640 [3] Segler MH, Preuss M, Waller MP (2018) Planning chemical syntheses with
641 deep neural networks and symbolic AI. Nature 555(7698):604–610, DOI 10.1038/
642 nature25978
- 643 [4] Schreck JS, Coley CW, Bishop KJ (2019) Learning retrosynthetic planning
644 through simulated experience. ACS central science 5(6):970–981, DOI 10.1021/
645 acscentsci.9b00055
- 646 [5] Liu B, Ramsundar B, Kawthekar P, Shi J, Gomes J, Luu Nguyen Q, Ho S, Sloane
647 J, Wender P, Pande V (2017) Retrosynthetic reaction prediction using neural
648 sequence-to-sequence models. ACS central science 3(10):1103–1113, DOI 10.1021/
649 acscentsci.7b00303

- 650 [6] Schwaller P, Petraglia R, Zullo V, Nair VH, Haeuselmann RA, Pisoni R,
651 Bekas C, Iuliano A, Laino T (2020) Predicting retrosynthetic pathways using
652 transformer-based models and a hyper-graph exploration strategy. *Chemical*
653 *science* 11(12):3316–3325, DOI 10.1039/C9SC05704H
- 654 [7] Coley CW, Rogers L, Green WH, Jensen KF (2017) Computer-assisted ret-
655 rosynthesis based on molecular similarity. *ACS central science* 3(12):1237–1245,
656 DOI 10.1021/acscentsci.7b00355
- 657 [8] Coley CW, Thomas III DA, Lummiss JA, Jaworski JN, Breen CP, Schultz V, Hart
658 T, Fishman JS, Rogers L, Gao H, et al (2019) A robotic platform for flow synthesis
659 of organic compounds informed by AI planning. *Science* 365(6453):eaax1566, DOI
660 10.1126/science.aax1566
- 661 [9] Gao H, Struble TJ, Coley CW, Wang Y, Green WH, Jensen KF (2018) Using
662 machine learning to predict suitable conditions for organic reactions. *ACS central*
663 *science* 4(11):1465–1476, DOI 10.1021/acscentsci.8b00357
- 664 [10] Schneider N, Lowe DM, Sayle RA, Tarselli MA, Landrum GA (2016) Big data
665 from pharmaceutical patents: a computational analysis of medicinal chemists’
666 bread and butter. *Journal of medicinal chemistry* 59(9):4385–4402, DOI 10.1021/
667 acs.jmedchem.6b00153
- 668 [11] Coley CW, Barzilay R, Jaakkola TS, Green WH, Jensen KF (2017) Prediction of
669 organic reaction outcomes using machine learning. *ACS central science* 3(5):434–
670 443, DOI 10.1021/acscentsci.7b00064
- 671 [12] Schwaller P, Gaudin T, Lanyi D, Bekas C, Laino T (2018) “Found in Transla-
672 tion”: predicting outcomes of complex organic chemistry reactions using neural
673 sequence-to-sequence models. *Chemical science* 9(28):6091–6098, DOI 10.1039/
674 C8SC02339E
- 675 [13] Qian WW, Russell NT, Simons CL, Luo Y, Burke MD, Peng J (2020) Integrating
676 deep neural networks and symbolic inference for organic reactivity prediction.
677 ChemRxiv DOI 10.26434/chemrxiv.11659563.v1
- 678 [14] Watson IA, Wang J, Nicolaou CA (2019) A retrosynthetic analysis algo-
679 rithm implementation. *Journal of cheminformatics* 11(1):1–12, DOI 10.1186/
680 s13321-018-0323-6
- 681 [15] Schwaller P, Vaucher AC, Laino T, Reymond JL (2021) Prediction of chemical
682 reaction yields using deep learning. *Machine learning: science and technology*
683 2(1):015,016, DOI 10.1088/2632-2153/abc81d
- 684 [16] Probst D, Schwaller P, Reymond JL (2022) Reaction classification and yield
685 prediction using the differential reaction fingerprint DRFP. *Digital discovery*
686 1(2):91–97, DOI 10.1039/D1DD00006C
- 687 [17] Ghiandoni GM, Bodkin MJ, Chen B, Hristozov D, Wallace JE, Webster J, Gillet
688 VJ (2019) Development and application of a data-driven reaction classification
689 model: comparison of an electronic lab notebook and medicinal chemistry liter-
690 ature. *Journal of chemical information and modeling* 59(10):4167–4187, DOI 10.
691 1021/acs.jcim.9b00537
- 692 [18] Schneider N, Lowe DM, Sayle RA, Landrum GA (2015) Development of a novel
693 fingerprint for chemical reactions and its application to large-scale reaction classi-
694 fication and similarity. *Journal of chemical information and modeling* 55(1):39–53,

- 695 DOI 10.1021/acs.jcim.5b00046
- 696 [19] Jaworski W, Szymkuć S, Mikulak-Klucznik B, Piecuch K, Klucznik T,
697 Kaźmierowski M, Rydzewski J, Gambin A, Grzybowski BA (2019) Automatic
698 mapping of atoms across both simple and complex chemical reactions. *Nature*
699 *communications* 10(1):1434, DOI 10.1038/s41467-019-09440-2
- 700 [20] Schwaller P, Hoover B, Reymond JL, Strobelt H, Laino T (2021) Extraction of
701 organic chemistry grammar from unsupervised learning of chemical reactions.
702 *Science Advances* 7(15):eabe4166, DOI 10.1126/sciadv.abe4166
- 703 [21] Liu T, Cao Z, Huang Y, Wan Y, Wu J, Hsieh CY, Hou T, Kang Y (2023) SynCluster:
704 Reaction Type Clustering and Recommendation Framework for Synthesis
705 Planning. *JACS Au* 3(12):3446–3461, DOI 10.1021/jacsau.3c00607
- 706 [22] Strieth-Kalthoff F, Sandfort F, Kühnemund M, Schäfer FR, Kuchen H, Glorius F
707 (2022) Machine learning for chemical reactivity: The importance of failed exper-
708 iments. *Angewandte Chemie International Edition* 61(29):e202204,647, DOI 10.
709 1002/anie.202204647
- 710 [23] Llanos EJ, Leal W, Luu DH, Jost J, Stadler PF, Restrepo G (2019) The explo-
711 ration of the chemical space and its three historical regimes. *Proc Natl Acad Sci*
712 *USA* 116:12,660–12,665, DOI 10.1073/pnas.1816039116
- 713 [24] Hawizy L, Jessop DM, Adams N, Murray-Rust P (2011) ChemicalTagger: A tool
714 for semantic text-mining in chemistry. *Journal of cheminformatics* 3:1–13, DOI 10.
715 1186/1758-2946-3-17
- 716 [25] Jablonka KM, Patiny L, Smit B (2022) Making the collective knowledge of chem-
717 istry open and machine actionable. *Nature Chemistry* 14(4):365–376, DOI 10.
718 1038/s41557-022-00910-7
- 719 [26] Nugmanov R, Dyubankova N, Gedich A, Wegner JK (2022) Bidirectional
720 Graphormer for Reactivity Understanding: neural network trained to reaction
721 atom-to-atom mapping task. *Journal of Chemical Information and Modeling*
722 62(14):3307–3315, DOI 10.1021/acs.jcim.2c00344
- 723 [27] Lin A, Dyubankova N, Madzhidov TI, Nugmanov RI, Verhoeven J, Gimadiev
724 TR, Afonina VA, Ibragimova Z, Rakhimbekova A, Sidorov P, et al (2022) Atom-
725 to-atom mapping: a benchmarking study of popular mapping algorithms and
726 consensus strategies. *Molecular Informatics* 41(4):2100,138, DOI 10.1002/minf.
727 202100138
- 728 [28] Nugmanov RI, Mukhametgaleev RN, Akhmetshin T, Gimadiev TR, Afonina VA,
729 Madzhidov TI, Varnek A (2019) CGRtools: Python library for molecule, reaction,
730 and condensed graph of reaction processing. *Journal of chemical information and*
731 *modeling* 59(6):2516–2521, DOI 10.1021/acs.jcim.9b00102
- 732 [29] Zhang C, Arun A, Lapkin A (2023) Completing and balancing database excerpted
733 chemical reactions with a hybrid mechanistic-machine learning approach. *Chem-*
734 *Rxiv* DOI 10.26434/chemrxiv-2023-hrgfw
- 735 [30] Ehrlich HC, Rarey M (2011) Maximum common subgraph isomorphism algo-
736 rithms and their applications in molecular science: a review. *Wiley Interdis-*
737 *ciplinary Reviews: Computational Molecular Science* 1(1):68–79, DOI 10.1002/
738 wcms.5

- 739 [31] Willett P, Barnard JM, Downs GM (1998) Chemical similarity searching. *Journal of chemical information and computer sciences* 38(6):983–996, DOI 10.1021/
740 ci9800211
- 741
- 742 [32] Willett P (2005) Searching techniques for databases of two- and three-dimensional
743 chemical structures. *Journal of Medicinal Chemistry* 48(13):4183–4199, DOI 10.
744 1021/jm0582165
- 745 [33] Stahl M, Mauser H (2005) Database clustering with a combination of fingerprint
746 and maximum common substructure methods. *Journal of chemical information
747 and modeling* 45(3):542–548, DOI 10.1021/ci050011h
- 748 [34] Gardiner EJ, Gillet VJ, Willett P, Cosgrove DA (2007) Representing clusters
749 using a maximum common edge substructure algorithm applied to reduced graphs
750 and molecular graphs. *Journal of chemical information and modeling* 47(2):354–
751 366, DOI 10.1021/ci600444g
- 752 [35] Boecker A (2008) Toward an improved clustering of large data sets using max-
753 imum common substructures and topological fingerprints. *Journal of chemical
754 information and modeling* 48(11):2097–2107, DOI 10.1021/ci8000887
- 755 [36] Raymond JW, Watson IA, Mahoui A (2009) Rationalizing lead optimization by
756 associating quantitative relevance with molecular structure modification. *Journal
757 of chemical information and modeling* 49(8):1952–1962, DOI 10.1021/ci9000426
- 758 [37] McGregor JJ, Willett P (1981) Use of a maximum common subgraph algorithm
759 in the automatic identification of ostensible bond changes occurring in chemical
760 reactions. *Journal of Chemical Information and Computer Sciences* 21(3):137–
761 140, DOI 10.1021/ci00031a005
- 762 [38] Fooshee D, Andronico A, Baldi P (2013) ReactionMap: An efficient atom-mapping
763 algorithm for chemical reactions. *Journal of chemical information and modeling*
764 53(11):2812–2819, DOI 10.1021/ci400326p
- 765 [39] Kawabata T, Nakamura H (2014) 3D flexible alignment using 2D maximum com-
766 mon substructure: dependence of prediction accuracy on target-reference chem-
767 ical similarity. *Journal of chemical information and modeling* 54(7):1850–1863,
768 DOI 10.1021/ci500006d
- 769 [40] Garey MR, Johnson DS (1979) *Computers and Intractability: A Guide to the
770 Theory of NP-Completeness*. W. H. Freeman, San Francisco
- 771 [41] Kawabata T (2011) Build-up algorithm for atomic correspondence between chem-
772 ical structures. *Journal of chemical information and modeling* 51(8):1775–1787,
773 DOI 10.1021/ci2001023
- 774 [42] Pomper P (1962) Lomonosov and the Discovery of the Law of the Conservation of
775 Matter in Chemical Transformations. *Ambix* 10(3):119–127, DOI 10.1179/amb.
776 1962.10.3.119
- 777 [43] Carruthers W, Coldham I (2004) *Modern Methods of Organic Synthesis*, Cam-
778 bridge Univ. Press, Cambridge, UK, chap Formation of carbon–carbon single
779 bonds, pp 1–104. DOI 10.1017/CBO9780511811494.003
- 780 [44] Landrum G (2013) Rdkit documentation. Release 1(1-79):4
- 781 [45] Kozen DC (1992) *The design and analysis of algorithms*, Springer, chap Depth-
782 first and breadth-first search, pp 19–24. DOI 10.1007/978-1-4612-4400-4_4

- 783 [46] Dalke A, Hastings J (2013) FMCS: a novel algorithm for the multiple MCS prob-
784 lem. *Journal of cheminformatics* 5(Suppl 1):O6, DOI 10.1186/1758-2946-5-S1-O6
- 785 [47] Raymond JW, Gardiner EJ, Willett P (2002) Rascal: Calculation of graph
786 similarity using maximum common edge subgraphs. *The Computer Journal*
787 45(6):631–644, DOI 10.1093/comjnl/45.6.631
- 788 [48] Chen T, He T, Benesty M, Khotilovich V, Tang Y, Cho H, Chen K, Mitchell
789 R, Cano I, Zhou T, et al (2015) Xgboost: extreme gradient boosting. R package
790 version 04-2 1(4):1–4
- 791 [49] Batista GE, Prati RC, Monard MC (2004) A study of the behavior of sev-
792 eral methods for balancing machine learning training data. *ACM SIGKDD*
793 *explorations newsletter* 6(1):20–29, DOI /10.1145/1007730.1007735
- 794 [50] Lemaître G, Nogueira F, Aridas CK (2017) Imbalanced-learn: A python tool-
795 box to tackle the curse of imbalanced datasets in machine learning. *J Machine*
796 *Learning Res* 18(17):1–5
- 797 [51] Andersen JL, Flamm C, Merkle D, Stadler PF (2016) A Software Package for
798 Chemically Inspired Graph Transformation. In: Echahed R, Minas M (eds) *Graph*
799 *Transformation, ICGT 2016*, Springer Verlag, Berlin, Heidelberg, D, *Lecture*
800 *Notes Comp. Sci.*, vol 9761, pp 73–88, DOI 10.1007/978-3-319-40530-8_5

801 **Supplementary Information**

802 **Comparison of the MCS Variants**

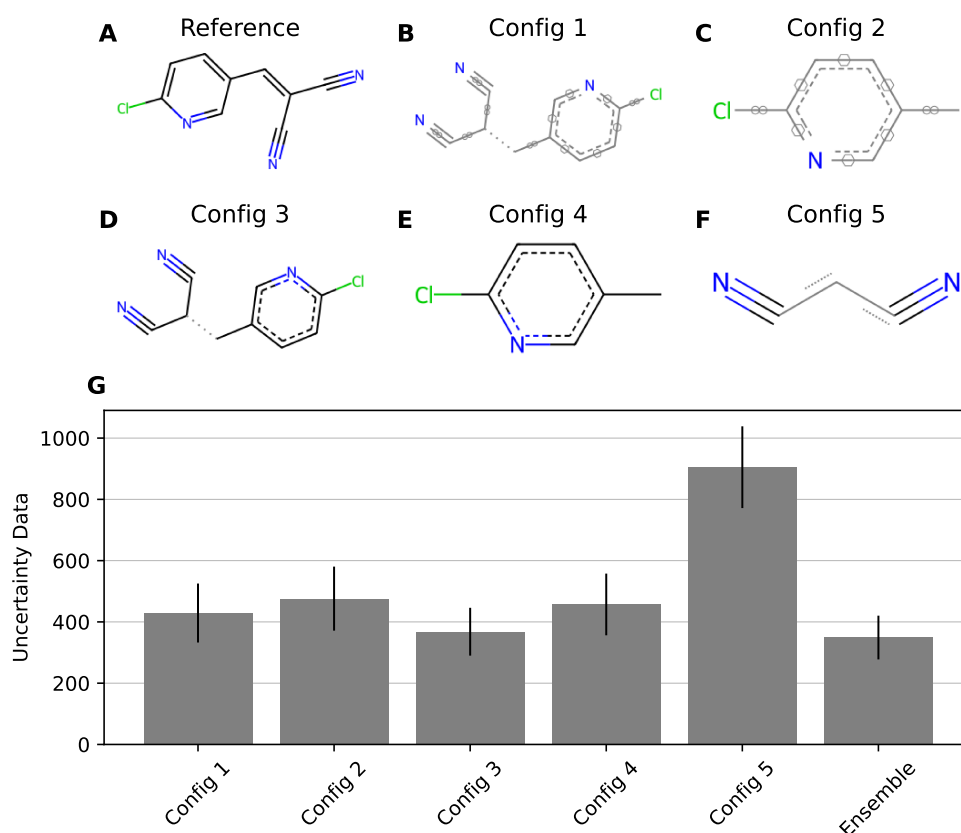


Fig. S1: Benchmarking analysis of MCS search configuration. (A) represents the reference molecules. (B-F) illustrate the MCS results from various configurations. (G) demonstrates the comparative analysis among different configurations and an ensemble method.

803 As described in the main text, the MCS problem was solved in several different
 804 versions (“configurations”), none of which is guaranteed to always identify the chem-
 805 ically correct common subgraph. We benchmarked the different variants and found
 806 that they are at least in part complementary. As depicted in Fig. S1, spanning panels
 807 A through F, three distinct cases of MCS were identified, where configurations 1 to 4
 808 were MCIS, while configuration 5 was MCES. Notably, the MCES approach demon-
 809 strated a capability to expedite the resolution of the NP-hard subgraph isomorphism

810 problem more efficiently than its MCIS counterpart. However, its performance effi-
811 cacy was suboptimal, a trend observable in Fig. S1G. This discrepancy is likely due
812 to the significant role of bond modifications in chemical reactions, highlighting the
813 dependence of the MCES search on bond-defined substructures. Remarkably, Config-
814 uration 3 achieved superior performance, disregarding bond order and complete rings,
815 excluding comparisons with ensemble methods.

816 These finds emphasize the well-known fact that any particular variant of the
817 graph-theoretical MCS problem does not always identify the chemically correct atom
818 correspondences between molecular graphs. The combination of multiple variations, as
819 implemented in the ensemble method, can achieve at least a moderate improvement,
820 Figure S1G. However, given the additional computational cost of computing multiple
821 MCS solutions, Configuration 3 appears to be best pragmatic choice given its perfor-
822 mance and reduced computational requirements. This observation that the ensemble
823 approach improved chemical correctness, albeit slightly, however, can serve as a natural
824 starting point for the development of an improved combinatorial atom-atom-mapping
825 method.

Table S1: Merge Rules; FG: Functional Group

Cond. <i>u</i>	Cond. <i>v</i>	Action <i>u</i>	Action <i>v</i>	Bond
O FG: Carbonyl	P Pattern: P=O	-	change_bond P=O to P-O	double
O FG: Carbonyl	P Pattern: !P=O	-	-	double
O FG: Enol, Alcohol, Phenol	P	-	-	single
S	X	-	-	no bond
N,O,X	N,O,X	-	-	no bond
*	*	-	-	single

Table S2: Expand Rules; FG: Functional Group; cut edge: *u - v*

Cond. <i>u</i>	Cond. <i>v</i>	FG	Expand
C	O	Ether	I
C	S	Thioether	I
C	O	Ester	O
C	S	Thioester	O
C	N	Amide	O
Mg, Zn, Si, B	*	*	O
O	!O, !N	*	O
N	!O, !N	*	O
C	C	*	O

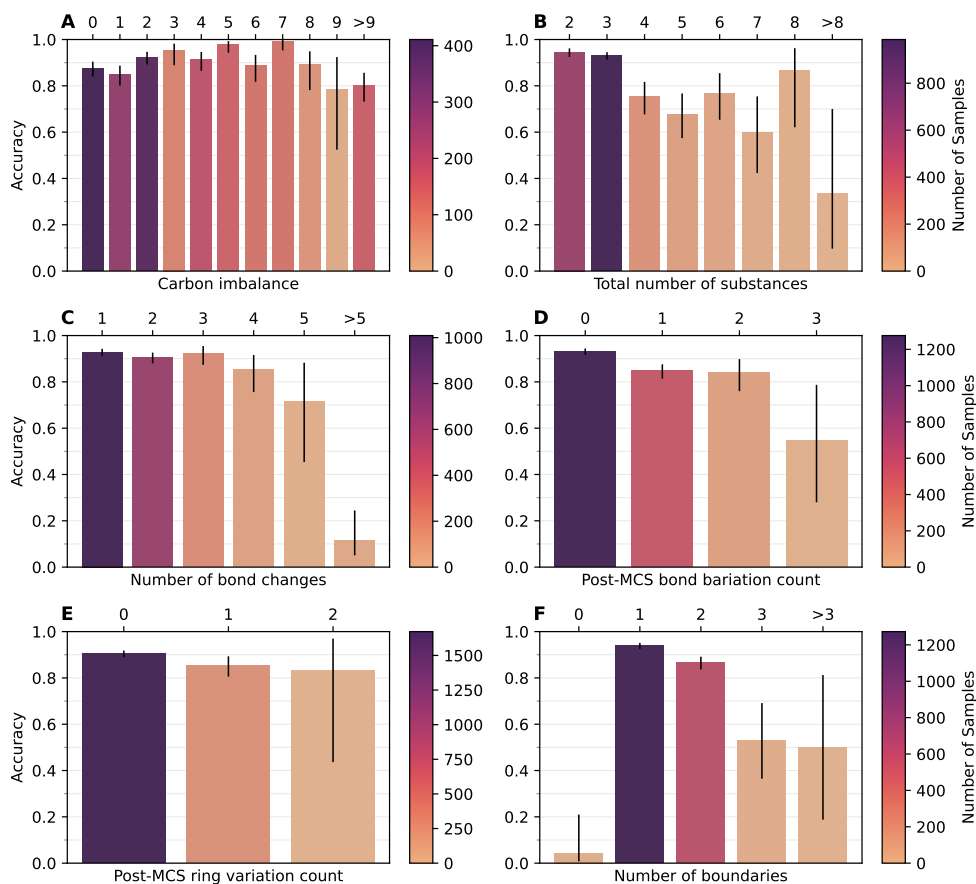


Fig. S2: Exploratory data analysis of MCS-based method performance. (A) Accuracy fluctuates slightly and declines when carbon imbalance exceeds seven. (B) The method performs best with less than four substances. (C) Accuracy drops with over five bond changes, indicating difficulty with rearrangement reactions. (D) Post-MCS bond differences between reactants and products show a decreasing trend similar to bond changes, with optimal performance below three. (E) Ring differences between reactants and products post-MCS show a minor decreasing trend with an increasing number of ring differences. (F) The detection of boundary atoms or reaction centers by MCS is crucial; the method fails without boundary atom detection and underperforms when the number exceeds two.

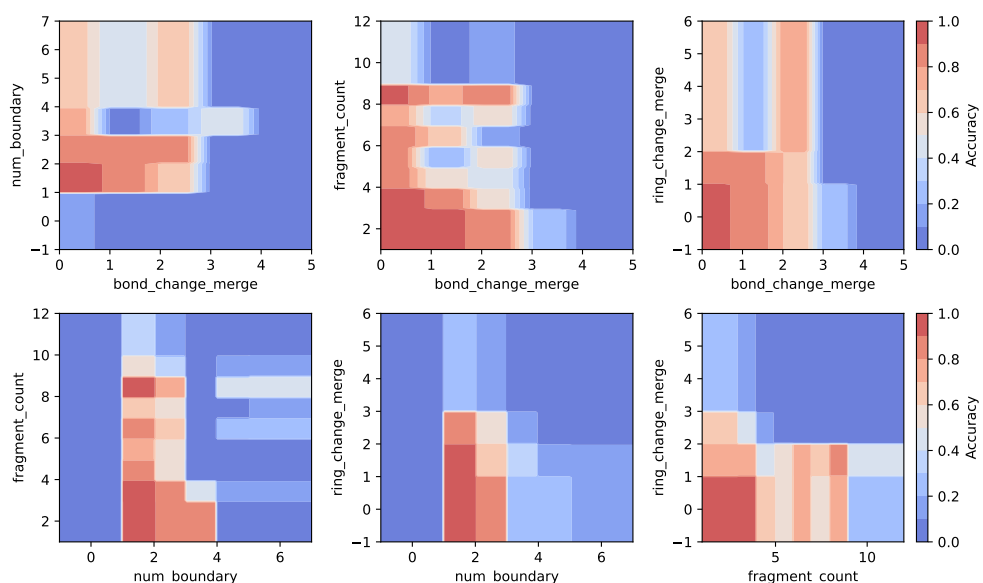


Fig. S3: Contour plots illustrate the confidence region formed by pairs of features. The warm colors in the contour plot represent regions of high confidence, indicating areas where our method demonstrates high accuracy. Conversely, the cool colors denote regions of lower confidence, reflecting areas where our method's accuracy is comparatively lower.

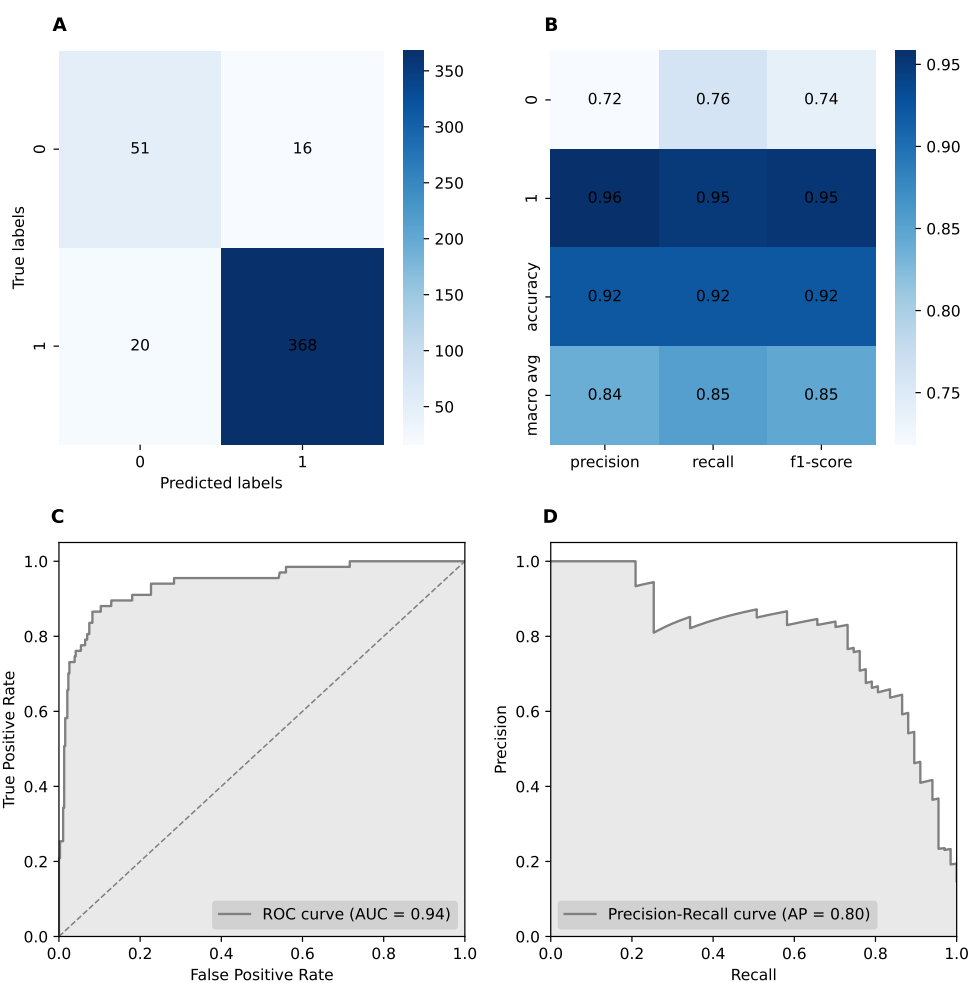


Fig. S4: Evaluation of model performance for a confidence level model using XGBoost and SMOTETomek. (A) The confusion matrix shows the number of actual versus predicted values. (B) The classification report provides performance metrics, including an F1 score of 0.91. (C) The ROC curve is presented with an AUC of 0.94. (D) The precision-recall curve is shown, with an average precision of 0.8.

Table S3: Library of substitution rules $\hat{r} \rightsquigarrow X_r$ for Section 2.2.2

X_r Formula	SMILES	\hat{r} Composition
O	[O]	{O: 1, Q: 0}
Cl ₂	ClCl	{Cl: 2, Q: 0}
N ₃ ⁻	[N-]=[N+]=[N-]	{N: 3, Q: -1}
H	[H]	{H: 1, Q: 0}
F ₂	FF	{F: 2, Q: 0}
Cl ₂	ClCl	{Cl: 2, Q: 0}
Br ₂	BrBr	{Br: 2, Q: 0}
I ₂	II	{I: 2, Q: 0}
H ⁺	[H+]	{H: 1, Q: 1}
Na ⁺	[Na+]	{Na: 1, Q: 1}
Li ⁺	[Li+]	{Li: 1, Q: 1}
K ⁺	[K+]	{K: 1, Q: 1}
Ca ²⁺	[Ca+2]	{Ca: 1, Q: 2}
Mg ²⁺	[Mg+2]	{Mg: 1, Q: 2}
Ba ²⁺	[Ba+2]	{Ba: 1, Q: 2}
Al ³⁺	[Al+3]	{Al: 1, Q: 3}
Zn ²⁺	[Zn+2]	{Zn: 1, Q: 2}
Cu ²⁺	[Cu+2]	{Cu: 1, Q: 2}
Cu ⁺	[Cu+]	{Cu: 1, Q: 1}
F ⁻	[F-]	{F: 1, Q: -1}
Cl ⁻	[Cl-]	{Cl: 1, Q: -1}
Br ⁻	[Br-]	{Br: 1, Q: -1}
I ⁻	[I-]	{I: 1, Q: -1}
N ₂	N#N	{N: 2, Q: 0}
O ₂	O=O	{O: 2, Q: 0}
S ²⁻	[S-2]	{S: 1, Q: -2}
H ₃ N	N	{N: 1, H: 3, Q: 0}
H ₂ O	O	{O: 1, H: 2, Q: 0}
H ₂ O ₂	OO	{O: 2, H: 2, Q: 0}
H ₄ N ⁺	[NH4+]	{N: 1, H: 4, Q: 1}
OH ⁻	[OH-]	{O: 1, H: 1, Q: -1}
NH ₃	N	{N: 1, H: 3, Q: 0}
NO ₂ ⁻	O=N[O-]	{N: 1, O: 2, Q: -1}
NO ₃ ⁻	[N+](=O)([O-])[O-]	{N: 1, O: 3, Q: -1}
NH ₂ ⁻	[NH2-]	{N: 1, H: 2, Q: -1}
SO ₄ ²⁻	[O-]S(=O)(=O)[O-]	{S: 1, O: 4, Q: -2}
PO ₄ ³⁻	[O-]P(=O)([O-])[O-]	{P: 1, O: 4, Q: -3}
SO ₃ ²⁻	[O-]S(=O)[O-]	{S: 1, O: 3, Q: -2}
IO ₃ ⁻	[O-]I(=O)=O	{I: 1, O: 3, Q: -1}
H ₃ NO	NO	{N: 1, O: 1, H: 3, Q: 0}
H ₄ NO ⁺	[NH3+]O	{N: 1, O: 1, H: 4, Q: 1}
B(OH) ₃	B(O)(O)O	{B: 1, O: 3, H: 3, Q: 0}
H ₃ BO ₂	B(O)(O)	{B: 1, O: 2, H: 3, Q: 0}
CO ₂	C=O	{C: 1, O: 2, Q: 0}
SOCl ₂	O=S(Cl)Cl	{S: 1, O: 1, Cl: 2, Q: 0}
H ₄ N ₂ O ₂ S	NS(N)=O=O	{N: 2, S: 1, O: 2, H: 4, Q: 0}
HClO ₃ S	O=S(=O)(O)Cl	{S: 1, O: 3, Cl: 1, H: 1, Q: 0}
B(OH) ₂ Cl	B(O)(O)Cl	{B: 1, O: 2, H: 2, Cl: 1, Q: 0}
B(OH) ₂ Br	B(O)(O)Br	{B: 1, O: 2, H: 2, Br: 1, Q: 0}
B(OH) ₂ I	B(O)(O)I	{B: 1, O: 2, H: 2, I: 1, Q: 0}
H ₂ ClNO ₂ S	NS(=O)(=O)Cl	{N: 1, S: 1, O: 2, Cl: 1, H: 2, Q: 0}

Table S4: Comprehensive Performance Metrics of the SynRBL

Dataset	Jaworski	Golden	Umb	Urnd	Udiff
Total number reactions	637	1851	540	803	1589
Number of unbalance reactions	335	1642	540	803	1589
Number of rule solved reactions	181	754	240	324	1134
Rule success rate (%)	89.6	93.55	97.96	99.69	96.1
Number of rule accurate reactions	179	752	239	322	1133
Rule accuracy (%)	98.9	99.73	99.58	99.38	99.91
Number of MCS solved reactions	127	721	298	479	451
MCS success rate (%)	82.47	81.19	99.33	100	99.12
Number of MCS accurate reactions	121	588	289	476	437
MCS accuracy (%)	95.28	81.55	96.98	99.37	96.9
All solved reactions	308	1475	538	803	1585
All success rate (%)	91.94	89.83	99.63	100	99.75
All accurate reactions	300	1340	528	798	1570
All accuracy (%)	97.40	90.85	98.14	99.38	99.05